The effect of web tension on calendering wrinkles and corrugations of coated foils

FU Zejun[1,a*], XU Zhutian[1,b] and PENG Linfa[1,c]

[1]Shanghai Jiao Tong University, No.800 Dongchuan Road, Minhang District, Shanghai, China

[a]fuzejun@sjtu.edu.cn, [b]zhutianxu@sjtu.edu.cn, [c]penglinfa@sjtu.edu.cn

Keywords: Lithium-Ion Batteries, Calendering Process, Wrinkles, Corrugations, Web Tension, Analytical Modelling

Abstract. Lithium-ion batteries have been widely used in energy storage for a range of applications from portable electronics, electric vehicles to power grids due to their high energy density, high power density and long cycle life. Calendering is a critical process in the manufacturing of lithium-ion batteries electrodes, which has a significant influence on volumetric energy density, long-term cycle stability, and electrochemical performance of lithium-ion batteries, etc. Wrinkles in the uncoated area and corrugations in the coated area of the electrode during the calendering process are serious problems in the industrial production of lithium-ion batteries, as shown in Fig. 1. Adjusting the web tensions has been a critical solution to mitigate these defects. However, large web tensions often lead to foil tearing, severe wrinkles, and high scrap rates, due to a lack of understanding of the wrinkling and corrugating behavior under different tension conditions. To cope with that, this stuedy aims to investigate the mechanism of wrinkling and the effect of web tension on the wrinkling of electrodes during calendering. Calendering experiments are carried out for lithium battery cathodes under different front and back tensions and the three-dimensional topographies of calendered electrodes are measured by a laser profiler. The corrugations of electrodes can be improved by the difference between the front and back tension, instead of the magnitude of the tension, and the tortuosity is reduced by 34.2% at a tension difference of 20 N, compared to that of 5 N. An increase of the tension difference leads to a linear increase of shear displacement δ, causing severe wrinkles in the uncoated area of electrodes. An analytical prediction model for the wrinkles during calendering is established based on shearing of the rectangular membrane and an electrode quality evaluation method for balancing wrinkles and corrugations is proposed. The determination of optimal web tension settings, with a tension difference of 17 N, is achieved to obtain the best quality calendered electrodes, which is in agreement with the experimental results. The method presented in this paper is helpful for the improvement of the production quality and efficiency of lithium battery electrodes.

Introduction

Lithium-ion batteries have been widely used in energy storage for a range of applications from portable electronics, electric vehicles to power grids due to their high energy density, high power density and long cycle life. The growing demand for high-performance and low-cost lithium-ion batteries results in challenges regarding refined understanding of engineering fundamentals and ingenuity in the electrode manufacturing process [1, 2]. The manufacturing process of lithium-ion batteries consists of slurry mixing, coating, drying, calendering, slitting, vacuum drying, and subsequent cell assembly and battery electrochemistry activation processes [3-5]. Calendering is a critical step in the fabrication of electrodes, which employs a high rolling load to compress the electrodes to a specified thickness. Calendering not only increases the volumetric energy density, but also enhances the electrical and thermal conductivity, long-term cycle stability, and electrochemical performance of the lithium-ion batteries [6-8].
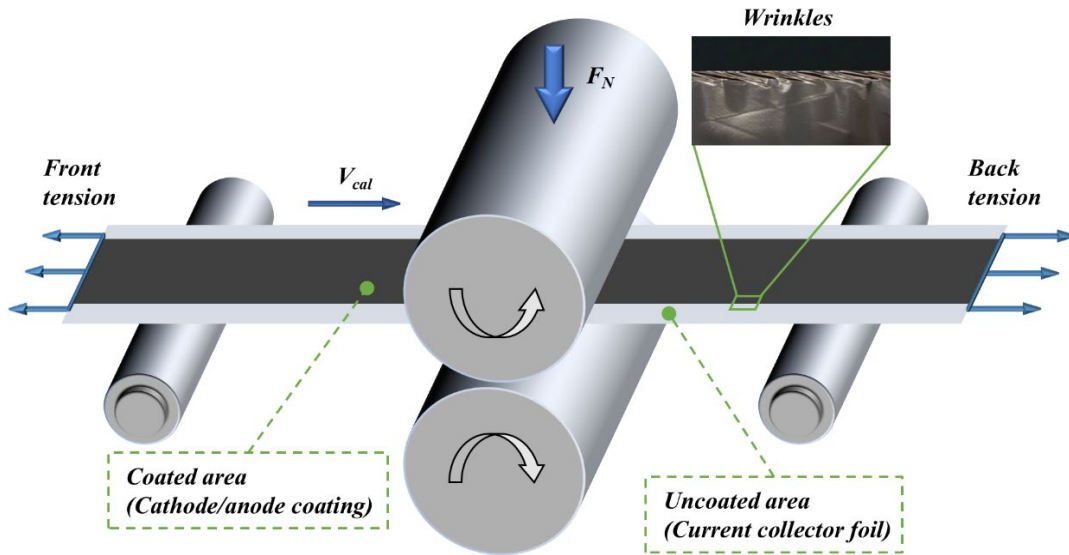
Fig. 1. Schematic of the calendering process including the appearance of electrode wrinkles.

The electrode is composed of a metal foil (aluminum for cathodes and copper for anodes) double-sided coated with a particulate composite (active ceramic powders for cathodes and graphite powders for anodes). Taking the cathode as an example, the thicknesses of the aluminum foil and single-side active coating are respectively 10-20 μm and 65-75 μm for commercial lithium-ion batteries, according to Zhu [9]. In the calendering process shown in Fig. 1, the electrodes are compacted to a required porosity by applying a line loads of more than 1000 N/mm between two rolls with a diameter of up to 1000 mm [10]. A high compaction pressure and thickness reduction rate are required to achieve a high volumetric energy density [11], which results in significant elongations of the electrodes. The elongation of the composite coating leads to evident corrugations in the coated area of the electrodes after calendaring. To eliminate those corrugations and maintain the flatness, web tension is applied to the front and back ends of the electrodes during the calendering process. In the existing processes, high web tension is used to reduce corrugations in the coated area, which at the same time leads to severe wrinkles in the uncoated area of the electrodes, as depicted in Figure 1. Those corrugations and wrinkles adversely affect the subsequent slitting, stacking, welding, electrolyte filling processes and cell performance [12, 13]. Besides, the increase of tension leads to tearing of ultra-thin foils more easily. Frequent failures thus occur on the production lines with the rolling speed up to 100 m/min, which significantly reduces productivity and increases costs.

A few studies have examined the wrinkles and corrugations of electrodes during calendering process. Guenther et al. divided calendering induced defects into three categories: geometrical, structural and mechanical ones, and evaluated the impact of them on the subsequent cell manufacturing processes. They found that corrugations in the coated area affect electrolyte filling, gripping and handling processes, while wrinkles in the uncoated area impair contacting and welding[12]. Mayer et al. investigated the corrugations and mechanical behavior of electrodes after calendering. The compaction rate, types of coating materials, and uncoated current collector foil were revealed to affect corrugations, while the web tension is identified to have little effect[13, 14]. This is attributed to the fact that, only cases with the same front and back tensions were involved in their study. Mayr et al. developed an in-line sensor-based process control method of the calendering process by applying in-line data acquisition for electrode thickness and surface topography, leading to a promising reduction of scrap and manufacturing costs [15]. Heating the rolls during calendering process has been investigated, the reduced line load and thus mechanical

stresses applied throughout the process are thought to be able to reduce the wrinkles of electrodes, especially at high line loads and high compaction rates [16-19].

Analytical and numerical simulation models of the calendering process of the calendering process are used as additions to experimental analysis and provide insights into the actual deformation of electrodes between two rolls [20]. Zhang et al. conducted tensile and compression experiments to obtain the constitutive properties of porous electrodes and identified the mechanism of failure behavior of electrodes by implementing the proposed constitutive models into finite element analysis.[21, 22]. Gupta et al. characterized the stress-strain relationship for a dry cathode active layer in lithium-ion batteries by means of U-shaped bending of single-side coated aluminum foils. A finite element model, with an elastic-ideally plastic material for the aluminum and an elastic material for the cathode active layer, was established to validate the evaluation of properties of cathode active layer [23]. Meyer et al. developed an exponential model between the applied line load and the achieved coating density by introducing compaction resistance. The relationship between mass loading, active materials and compaction resistance was established [24, 25]. Zhu et al. obtained the mechanical properties of anode and cathode coatings by compression tests in a specially designed aluminum mold. The sequence of deformation and failure of various components of lithium-ion batteries under mechanical loadings were simulated by employing the Drucker-Prager/Cap plasticity model in finite element model [9, 26]. Sahraei et al. obtained the stress-volumetric strain curve from the uniaxial compression experiment of the cell and modeled the cell by finite element method using a crushable foam material and predicted the load-displacement response[27, 28]. Besides analytical and finite element modeling, the numerical simulation of the calendering process by means of the discrete element method (DEM) has given deeper insight into the compaction of electrodes[29-33]. However, the scale of simulation models for DEM is usually only a few hundred micrometers, whereas the battery modeling involves six orders of magnitude levels in length[27], which limits its applicability in the study of electrode manufacturing processes.

According to the above reviews, wrinkles and corrugations of the electrodes during calendering process are critical problems during the manufacturing of lithium-ion batteries, which attract both industrial and academic attentions. However, a detailed understanding of those defects and process design methods are still lacking. In practical production, the mitigation of wrinkles and corrugations relies on experiences, resulting in high labor intensity, long commissioning time, waste of electrode materials and high scrap rates. In this paper, Calendering experiments of electrodes for lithium-ion batteries under different tension settings are first carried out. Then, a laser sensor-based measurement and evaluation method of electrode wrinkles and corrugations is developed. The mechanism of electrode wrinkles and corrugations during calendering process and the effect of tension on them are explained. Finally, an analytical prediction model for the wrinkles and an evaluation method for the quality of the calendered electrodes is established. The selection of tension settings is accomplished using this model and an agreement with the experimental results is achieved. The method presented in this paper is helpful for the improvement of the production quality and efficiency of the calendering process for lithium-ion batteries.

Experiments

Materials. The uncalendered $LiNi_{0.5}Co_{0.2}Mn_{0.3}O_2$ (NCM523) cathode is manufactured by MTI KJ GROUP, containing 95.5% active material, 2.5% carbon black and 2% binder, with a total thickness of about 160 μm. The active material is coated on both sides of a 16 μm thick aluminum foil at a surface mass loading of 29.3 mg/cm^2. The width of the coated active material is 200 mm and the width of the uncoated current collector foil is 40 mm.

Experimental setup. In the calendering process, the electrodes are continuously compacted with a two-roller calender MSK-2300A-E as shown in Fig. 2(a). The diameter and the width of calender rolls are 200 mm and 300 mm respectively. The electrodes after coating and drying are calendered

at ambient temperature and a rolling speed of 2 m/min. The applied line load of the calender is 1250 N/mm and the electrodes are compacted from an initial density of 2.03 g/cm^3 to a compaction one of 2.87 g/cm^3.
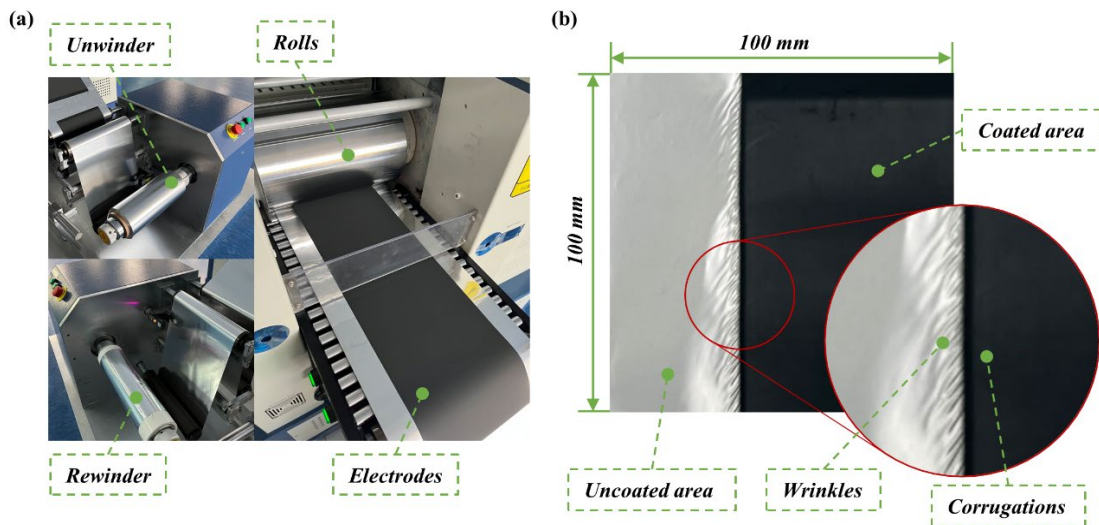

Fig. 2. Experimental procedures: (a) electrodes calendering systems; (b) images of electrodes after calendering.

As mentioned above, this study focuses on the effect of the front and back tensions on the electrode wrinkles and corrugations. An experiment with no tension applied is employed for comparison. After that, the complete experiments are designed to investigate the effect of front and back tensions. The front tension is designed from 5 to 20 N with an interval of 5 N, and the difference between the front and back tensions is designed from 0 to 20 N with an interval of 5 N. In addition, the uncoated current collector is thought to hinder electrode deformation according to Mayer [13], two different collector width, i.e. 0 and 40 mm, are discussed to investigate its effect on wrinkles and corrugations. The values of front and back tensions could be adjusted by the unwinder and rewinder presented in Fig. 2(a). Three electrodes are calendered for each experimental condition. As depicted in Fig. 2(b), all electrodes are cut into sheets with a length of 100 mm after calendering to enable the measurement of electrode wrinkles and corrugations.

Three-dimensional scanning of the calendered electrodes is performed using a Keyence LJ-X8020 laser profiler mounted on a three-axis motion stage. The laser sensor has a measuring range of 8 mm along the width and 4 mm along the height, and the accuracy of the sensor is 0.3 μm. The laser sensor acquired the height profiles of the electrodes along the x-direction (which is perpendicular to the running direction) at a frequency of 1000 Hz and the speed of the motion stage along the y-direction (which is in the running direction) is 10 mm/s. The three-dimensional topographies of the electrodes after calendering are obtained by stacking the acquired height profiles with the interval to 0.01 mm.

Results and discussion

Measurement of wrinkles and corrugations. Wrinkles in the uncoated area and corrugations in the coated area are geometric defects that coexist on calendered electrodes. The quantification of wrinkles and corrugations need to be conducted for the sake of evaluating the degree of geometrical defects of the calendered electrodes. As shown in Fig. 3, based on the three-dimensional scanning results of the calendered electrodes, two height profiles at a distance of ±1mm from the junction of the coated and uncoated areas are extracted along the rolling direction, as illustrated by the dash lines l_1 for the coated area and l_2 for the uncoated area, respectively.

The wavelength of corrugations in the coated areas is found in the centimeter range. The following data processing procedure is conducted to capture the major corrugation features after calendering: (1) smoothing: Savitzky-Golay filtering with a smoothing window of 300 data points is carried out to remove the minor fluctuations; (2) elimination of the overall electrode inclination after cutting: a straight line connecting the start and end points, which represents the overall inclination of the electrodes, is subtracted from the smoothed data. After those, the cross-section curve of corrugations in the coated area can be obtained as shown in Fig. 3(a). In order to avoid excessive random errors caused by the direct use of the maximum value of the height of corrugations, the degree of tortuosity ΔC, is proposed as an evaluation index of the corrugations in the coated area. ΔC is the difference between the total length C of the coated area in the calendered electrodes and the length C_0 scanned by the laser sensor along the rolling direction, and the value of C_0 is 100mm.
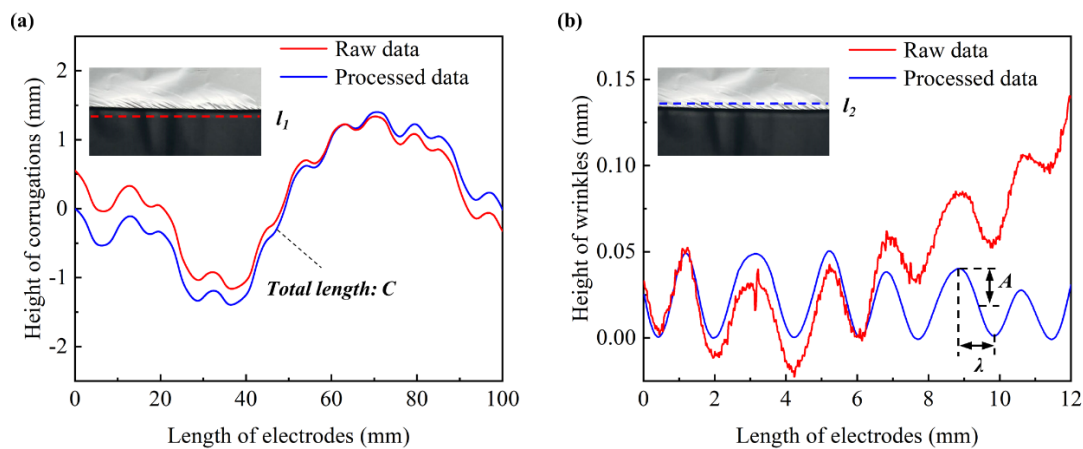

Fig. 3. Evaluation of calendered electrodes: (a) corrugations in the coated area; (b) wrinkles in the uncoated area of electrodes.

In the uncoated area, short and dense wrinkles in the collector foil are the main geometrical defects. As illustrated in Fig. 3(b), the wavelength and amplitude of wrinkles in this region are in the millimeter range. Both the overall inclination of the electrode and the corrugations in the coated area affect the measurement results. To capture the wrinkles data, the overall inclination of the electrode and the centimeter-range corrugations of the coated area need to be eliminated from the raw data. Therefore, the following processing procedure is conducted for the uncoated area: (1) smoothing: Savitzky-Golay filtering with a smoothing window of 100 data points is performed to smooth the data; (2) elimination of the overall inclination of the electrode and corrugations: a spline curve fitted by the valley points of each wrinkle, instead of a straight line, is subtracted from the smoothed data. After that, the cross-section curve of wrinkles can be obtained and the ratio R of amplitude A to half wavelength λ of the wrinkles is employed as an evaluation index aimed at evaluating the severity of wrinkles in the uncoated area.

Mechanisms of wrinkles and corrugations. To investigate the cause of wrinkles and corrugations in the calendering process of the electrodes, the results of experiments #1, #2, #8, and #11 are compared. The height profiles of the coated area and uncoated areas of the electrodes along the rolling direction under four different conditions, i.e. without uncoated current collector, no front and back tensions, equal front and back tensions, and greater back tension, are obtained.

As illustrated in Fig. 4(a), in the absence of the uncoated collector, the coated area of electrodes elongated after calendering and the coated area is not corrugated. In comparision with the case #2, where the uncoated collector is present, significant corrugations is observed in the coated area of

electrodes. That is because the foil in the uncoated area is not in contact with the rolls and thus not elongated after calendering process. As a result, the foil hindered the elongation of the coated area, which results in out-of-plane bending and deformation of the coated area. Due to the elongation mismatch between the coated and uncoated areas, corrugations in the coated area occurred. However, if the uncoated area is removed, the elongation of the coated area is not restricted, leading to the elimination of the corrugations, as shown in Fig. 4(c).
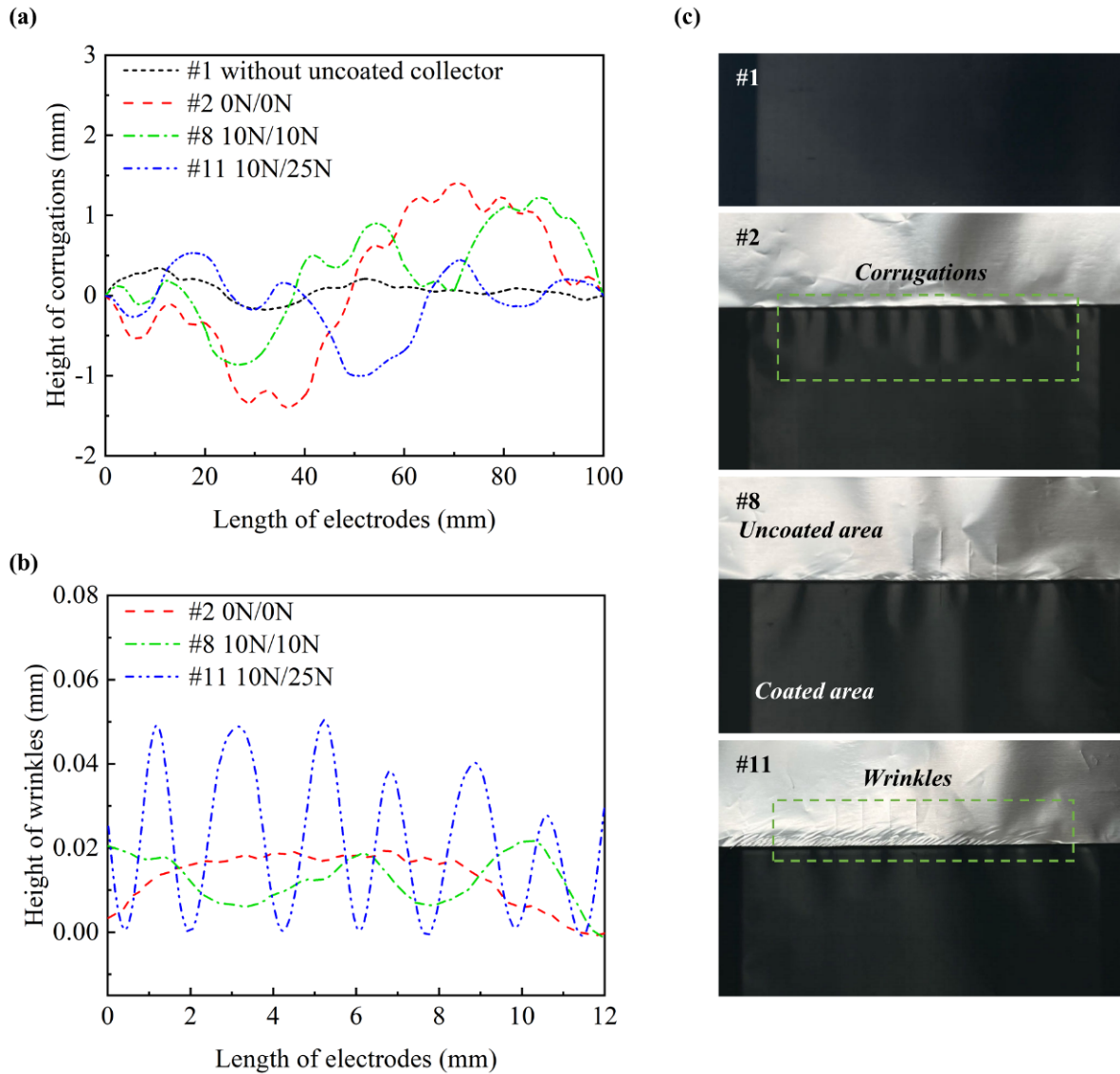

Fig. 4. Height profiles of electrodes under different conditions: (a) corrugations in coated area; (b) wrinkles in uncoated area; (c) the photographs of wrinkles and corrugations after calendering.

In the presence of an uncoated collector, the front and back tensions have significant effect on the wrinkles and corrugaitons of the electrodes. As shown in Fig. 4(a), when no front and back tensions applied, evident out-of-plane corrugations can be observed in the coated area. Meanwhile, the millimeter-range wrinkles is not significant. By increasing both the front and the back tensions to 10 N, similar corrugations and little wrinkles is observed in the coated and uncoated areas, respectively. Those observations are consistent with the results reported in the literature[34].

On the other hand, when keeping the front tension at 10 N while increasing the back tension to 25 N, the geometrical defect patterns of the electrodes changed significantly. The tortuosity of the corrugations in the coated area, which can be evaluated by the value of ΔC as described above, is reduced from 0.36 to 0.27 mm, compared to the case that the front and back tensions are equal. Meanwhile, as shown in Fig. 4(b) and (c), evident wrinkles in the uncoated area also appeared. Short and dense wrinkles appeared in the junction area near the uncoated side at an inclination angle of approximately 30 degrees to the direction of rolling.

In summary, increasing the front and back tensions simultaneously has little improvement effect and only the difference between the front and back tensions is the main parameter affecting the corrugations in the coated area and the wrinkles in the uncoated area. That is because the coated area of the electrode is elongated in the rolling direction after passing through the roll gap, and the back tension acts on the uncoated area that is not elongated, resulting in the collector foil being stretched backward. Thus, the difference in displacement between the two areas decreased and the hindering effect of the uncoated area on the elongation of the coated area is alleviated, thereby the flatness of the coated area is improved. At the same time, the uncoated area is stretched backwards to form evident wrinkles at the coating edge. In the cases where no tension is applied, the front and back tensions are increased simultaneously or the front tension is greater than the back tension, there is no backward stretching effect on the uncoated collector, therefore there is almost no effect on the improvement of the geometric defects of the electrodes.

Effect of web tension. To elaborate the effect of tension on the wrinkles and corrugations of the electrodes, the evaluation index ΔC for the coated area and the ratio of amplitude to half wavelength R, are obtained for all experiments. The experimental results showed that the tension difference between the front and back tensions affected the geometrical defects, instead of the magnitude of them. As shown in Fig. 5(a), when the tension difference remained 0 N and the front tension is 5 N, 10 N, 15 N, and 20 N, respectively, the increase of the front tension had little effect on ΔC. On the other hand, by controling the front tension a constant of 5 N, the tortuosity of corrugations decreased with the increase of the tension difference. As depicted in Fig. 5(b), with the tension difference increased from 5 to 20 N, the value of ΔC decreased from 0.38 to 0.25 mm, for a reduction of 34.2%.
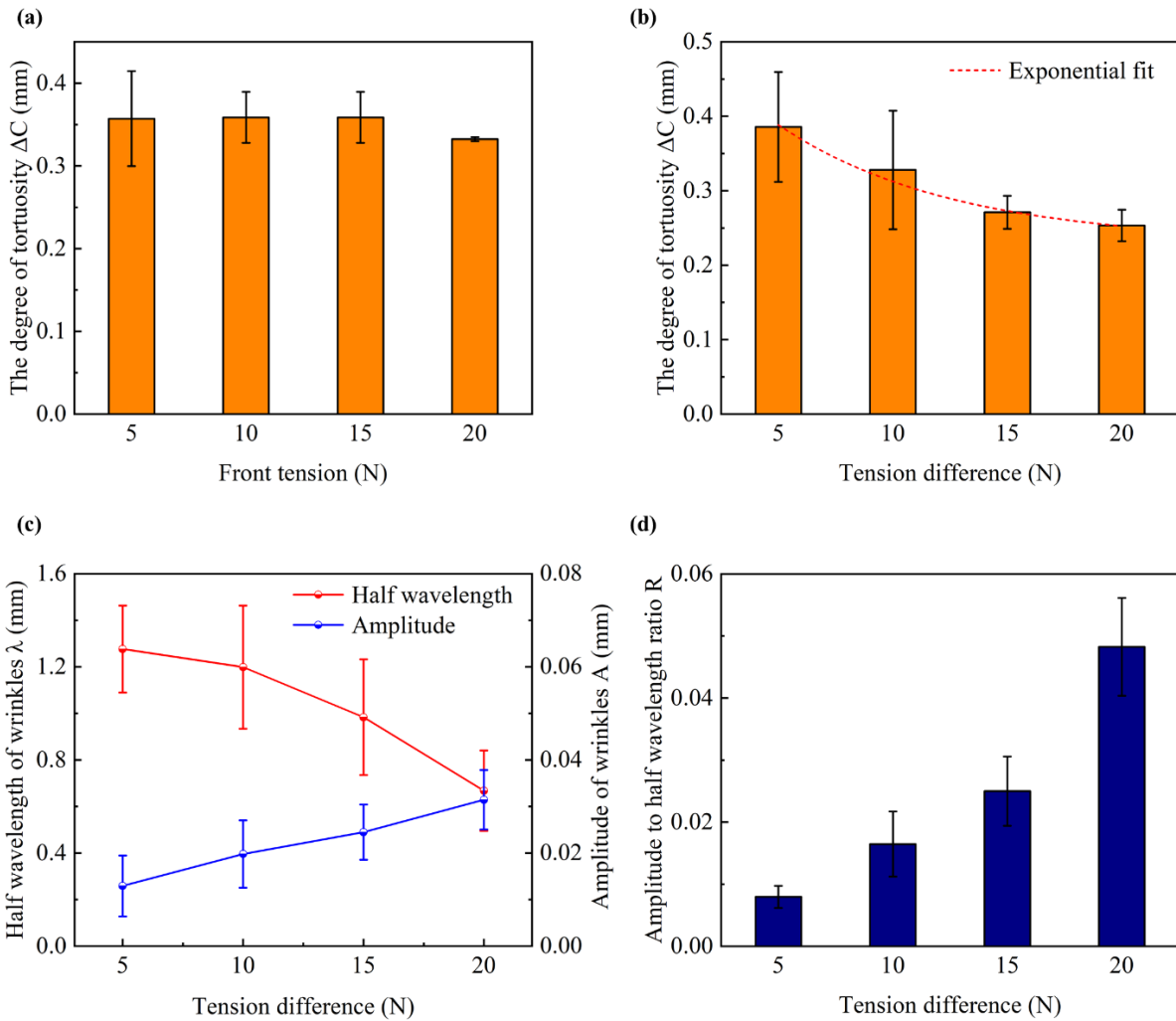
Fig. 5. Effect of the web tension, on corrugations: (a) front tension equals back tension; (b) front tension is 10 N, and the tension difference increased; on the half wavelength and amplitude (c), and the ratio of amplitude to half wavelength (d) of wrinkles at a front tension of 10 N.

As illustrated in Fig. 5(c), the height profiles of wrinkles in the uncoated area of the electrodes are obtained with different tension differences while making the front tension constant at 10 N. As the tension difference increased, the half wavelength of the wrinkles decreased while the amplitude increased. That leads to the difficulty of elastic recovery of the wrinkles and permanent deformation of the collector foil after the cutting process of the electrodes, which in turn affects subsequent processes of stacking, packaging and electrolyte filling in the production of lithium-ion batteries. As shown in Fig. 5(d), the effect of the tension difference on the amplitude-half wavelength ratio R of wrinkles is obtained. The increase in the difference between the front and back tensions led to a significant increase in the ratio R and more severe the wrinkles in the uncoated collector. That is due to an increased displacement difference between the coated and uncoated areas along the rolling direction induced by a larger tension difference.

As mentioned above, the corrugations and wrinkles of the electrodes after calendering are due to the mismatch of displacement between the coated and uncoated areas. To measure the difference in shear displacement, several grid lines are scribed on the surface of the uncalendered electrodes using a scribing needle and the 3D topographies of the electrodes are recorded before and after calenderging using a laser sensor described in Experimental setup. As shown in Fig. 6, the difference in shear displacement δ between the coated and uncoated areas is obtained by comparing

the deformation of the grid lines along the rolling direction before and after calendering. The shear displacement difference δ increased with the increasing tension difference T_d, which can be described by a linear relationship:
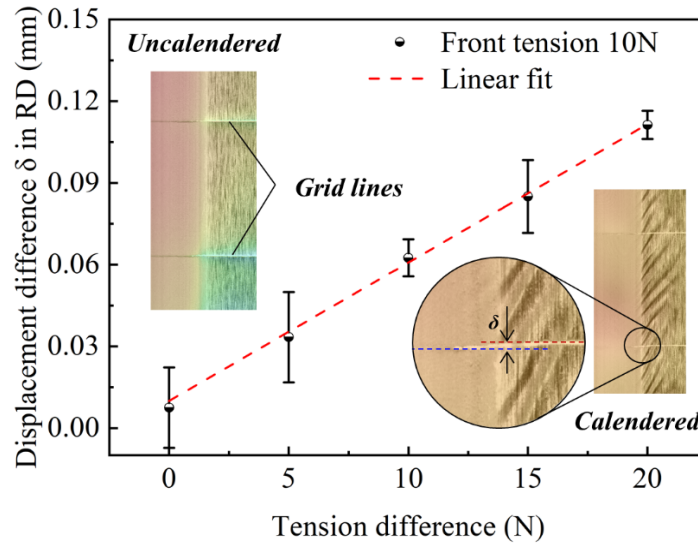
$$\delta = 0.01 + 0.00508 T_d \qquad\qquad (1)$$

Fig. 6. Relationship between shear displacement and tension difference.

Modeling and optimization

Based on the results obtained above, the difference between the front and back tensions is the key parameter affecting the corrugations and wrinkles of the electrodes. The preferred tension settings need to be selected to balance the corrugations in the coated area and wrinkles in the uncoated area, to obtain a better quality of calendered electrodes. Thus, an analytical model for predicting wrinkles is developed to determine the optimal web tension parameters.
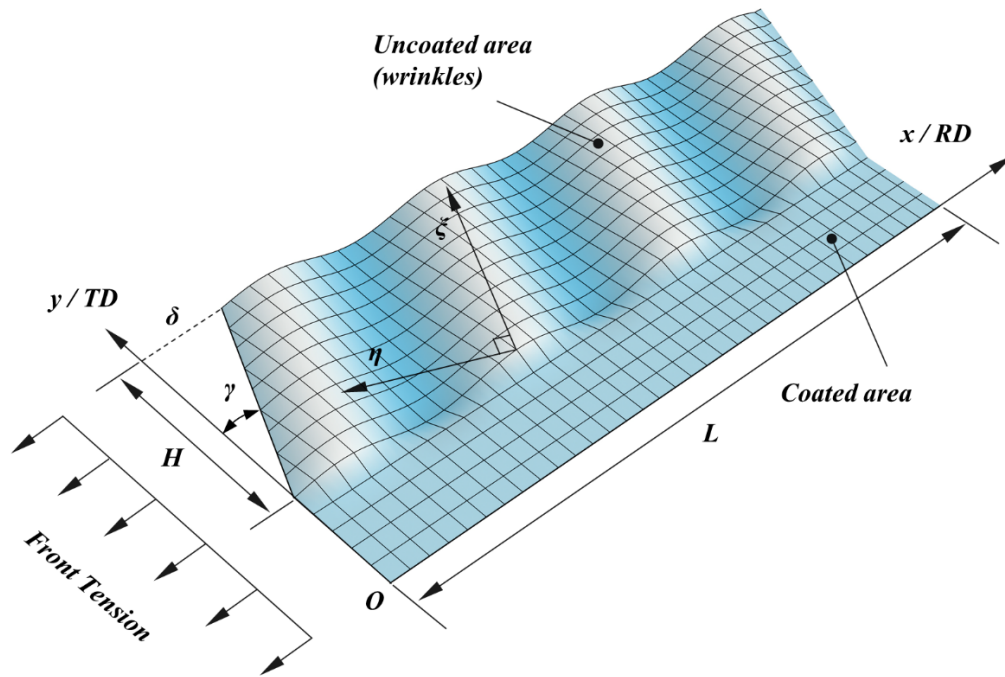
Fig. 7. Analytical model of shear wrinkling in the uncoated area of electrodes.

The following assumptions are made for the developed model: Firstly, linear elasticity, small deformations and homogeneity of the material are assumed. Secondly, the collector foil is assumed to be subjected to a uniform transverse in-plane displacement along the coating edge. Finally, the wrinkles are assumed to be parallel, evenly spaced, of uniform length, and inclined at 35° to the rolling direction, on the basis of experimental observations of wrinkles after calendering. The description of analytical model based on the bifurcation theory of thin-plate is shown in Fig. 7, the uncoated area of the electrode can be treated as a rectangular membrane with a width of H, the difference in displacement of coated and uncoated areas along the rolling direction is described by δ, and the shear angle γ, which can be calculated by $\gamma = \pi/180 \cdot arctan(\delta/H)$.

Referring to the analytical model for predicting wrinkles in rectangular membrane proposed by Wang [35], the initially flat collector foil deformed into a doubly curved shape, a model describing the wrinkled surface can be established using the coordinate systems ξ and η. ξ is parallel to the wrinkle direction and η is perpendicular to it.

The length of the model is kH, $k = 1/sin(35\pi/180)$ and the width is λ, the out-of-plane displacement function is configured as:

$$w = A\sin\frac{\pi\eta}{\lambda}\sin\frac{\pi\xi}{kH} \tag{2}$$

The uniaxial stress in the wrinkled region can be expressed as:

$$\sigma_\xi = E\gamma + \frac{\pi^2 E h^2}{12\lambda^2(1-v^2)} \tag{3}$$

where E is the Young's modulus with a value of 70 GPa, v is the Poisson's ratio with a value of 0.33 [28] and h refers to the thickness of the collector foil.

The critical wrinkling stress σ_η acting perpendicular to the wrinkles is assumed to equal the stress required to buckle a simply-supported, infinitely wide plate of length λ:

$$\sigma_\eta = -\frac{\pi^2 E h^2}{12\lambda^2(1-v^2)} \tag{4}$$

The force equilibrium relationship along the out-of-plane direction of the membrane can be expressed as:

$$\sigma_\xi k_\xi + \sigma_\eta k_\eta = 0 \tag{5}$$

where k_η and k_ξ are two curvatures of the surface and they are determined by Eq. (2). According to Eq. (2)-Eq. (5), the half wavelength λ of wrinkles of a rectangular collector foil subject to transverse in-plane shear displacement δ, as shown in Fig. 7, can be predicted by:

$$\lambda^2 = \frac{(kH\pi h)^2}{24\gamma(1-v^2)}[\sqrt{\frac{1}{(kH)^4} + \frac{48\gamma(1-v^2)}{(kH\pi h)^2}} - \frac{1}{(kH)^2}] \tag{6}$$

The total strain in the η direction is $-\gamma$, while the material strain in this direction is $-v\gamma$. The difference between the two is the "geometric strain":

$$\varepsilon_G = -\frac{\pi^2 A^2}{4\lambda^2} = -\gamma(1-v) \tag{7}$$

Thus, the amplitude of wrinkles can be solved from Eq. (6) and Eq. (7):

$$A = \frac{2\lambda\sqrt{\gamma(1-v)}}{\pi} \tag{8}$$

It should be noted that the accuracy of the amplitude prediction is not enough due to several simplified assumptions are used in the process of deriving the analytical model, such as linear elasticity, small deformations, etc. Based on the results of experiments, a modified value A_0 is subtracted, which has a value of 0.03, from the predicted value of amplitude to eliminate deviations resulting from simplified assumptions.
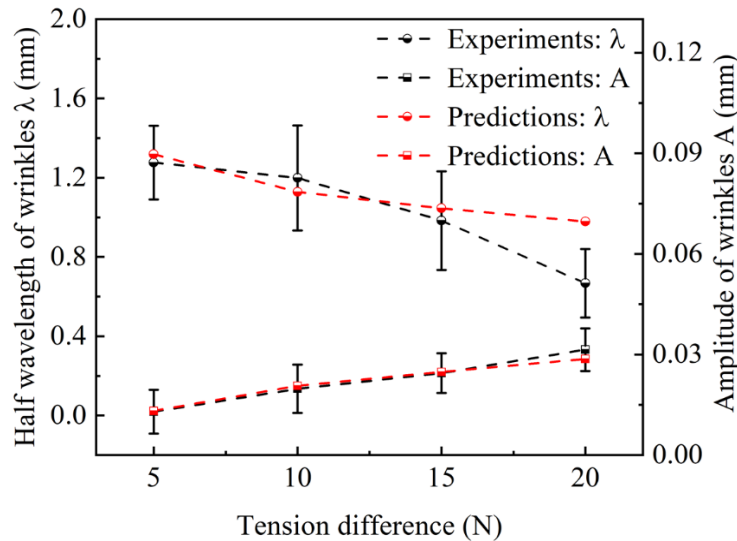

Fig. 8. Prediction of wrinkles: experimental and predicted results under different tension differences.

According to the analytical model for the prediction of wrinkles in the uncoated area of the electrodes, the half wavelength and amplitude of wrinkles are calculated using Eq. (6) and (8) at a

front tension of 10 N and a tension difference of 5 N, 10 N, 15 N, and 20 N, as shown in Fig. 8. It should be noted that, the predicted results are in agreement with the experimental results, except at the point where T_d is 20 N. The uncoated area is no longer in the elastic range as assumed and thus the wavelength of wrinkles is overestimated when the great tension difference is too large. However, large tension differences should be avoided in production, which may lead to tearing of the electrodes.

As for corrugations in the coated area, as depicted in Fig. 5(b), the improvement effect of the tortuosity ΔC in the coated area gradually tended to be constant when the tension difference continued to increase, which can be described by an exponential curve:

$$\Delta C = 0.23 + 0.304 \exp(-\frac{T_d}{7.62}) \tag{9}$$

where T_d is the difference between front and back tensions.

Both the corrugations in coated area and wrinkles in uncoated area have a detrimental effect on the quality of electrodes[12]. In order to find optimal settings of the web tension, an evaluation index I for the overall quality of calendered electrodes is established:

$$I = \alpha \Delta C + (1-\alpha)R \tag{10}$$

the relationship between ΔC and T_d can be obtained by Eq. (9). R is the ratio of amplitude to half wavelength, the relationship between R and T_d can be obtained by Eq. (1), Eq. (6) and Eq. (8). α is the weight, and its value is set to 0.2, based on expert consultations. The value of I is calculated for a range of tension differences T_d using Eq. (10). As illustrated in Fig. 10(a), the predicted minimum value of I is 0.0735, achieved at a T_d value of 17 N, at which point the best electrode quality is theoretically available.
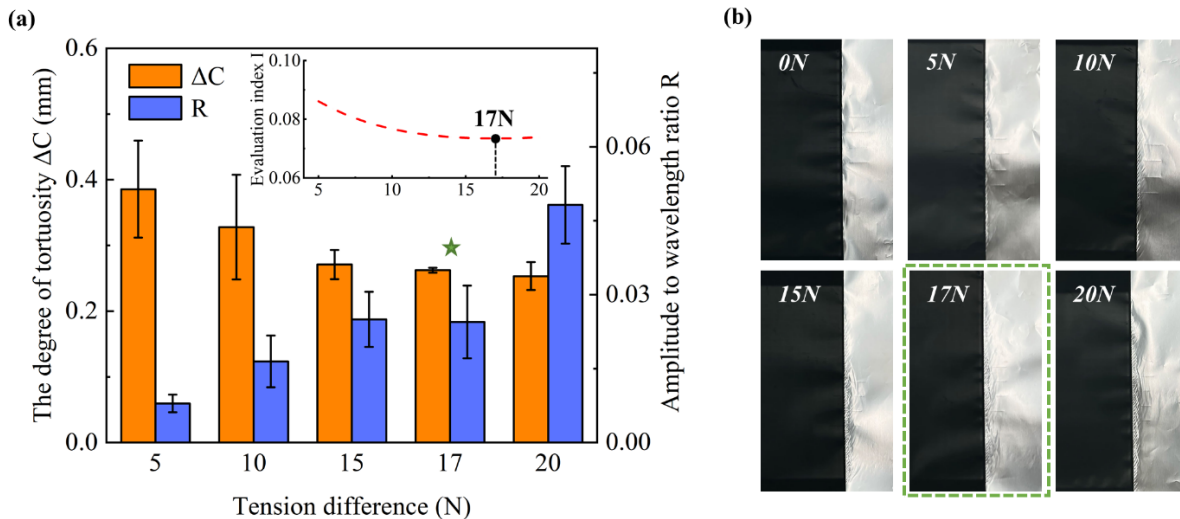

Fig. 9. Validation of the selected tension settings: (a) ΔC and amplitude to half wavelength ratio R of calendered electrodes; (b) photographs recording the appearance of calendered electrodes, under different tension differences.

To validate the previously chosen tension settings, experiments on electrode calendering at a tension difference T_d of 17 N are carried out additionally. As shown in Fig. 9(a), a comparison with the other four groups showed that, the corrugations in the coated area (described by the value of ΔC) are improved to a large extent and continued increase in the value of T_d did not improve it further, while the wrinkles in the uncoated area (described by the value of R) are limited to a relatively low level. From the appearance of the electrode after calendering, shown in Fig. 9(b),

the flatness of the electrodes is optimized at T_d value of 17 N as compared to the other four groups, with both wrinkles in the uncoated area and corrugations in the coated area considered, which is consistent with previous predictions.

Conclusion

The effect of web tension is clarified via both experiments and analytical modeling to explore the wrinkles and corrugations of electrodes during calendering process. Calendering experiments of cathode electrodes of lithium-ion batteries under different tension settings are carried out. The measurement and data processing methods of corrugations in the coated area and wrinkles in the uncoated area are also developed. The optimal tension difference T_d is determined by employing the proposed evaluation index of geometrical defects of calendered electrodes. The following conclusive remarks can be drawn:

(1) The tension difference between the front and back tensions is the key parameter to determine the wrinkles and corrugations of calendered electrodes. Corrugations in the coated area can be mitigated while wrinkles in the uncoated area become more evident by increasing the tension difference.

(2) An analytical prediction model for the wrinkles after calendering is established based on shearing of the rectangular membrane and an evaluation method for the quality of the calendered electrode is developed to balancing the effects of wrinkles and corrugations.

(3) The determination of the web tension parameters to improve the quality of calendered electrodes is achived at T_d of 17 N and the predicted results are consistent with the experimental results.

Acknowledgements

References

[1] W.B. Hawley, J. Li, Electrode manufacturing for lithium-ion batteries—Analysis of current and next generation processing, J. Energy Storage 25 (2019) 100862. https://doi.org/10.1016/j.est.2019.100862

[2] J. Li, J. Fleetwood, W.B. Hawley, W. Kays, From Materials to Cell: State-of-the-Art and Prospective Technologies for Lithium-Ion Battery Electrode Processing, Chem. Rev. 122 (2022) 903-56. https://doi.org/10.1021/acs.chemrev.1c00565

[3] J. Xiao, F. Shi, T. Glossmann, C. Burnett, Z. Liu, From laboratory innovations to materials manufacturing for lithium-based batteries, Nat. Energy 8 (2023) 329-339. https://doi.org/10.1038/s41560-023-01221-y

[4] J. Li, Z. Du, R.E. Ruther, S. Jin, L.A. David, K. Hays, M. Wood, N.D. Phillip, Y. Sheng, C. Mao, S. Kalnaus, C. Daniel, D.L. Wood III, Toward Low-Cost, High-Energy Density, and High-Power Density Lithium-Ion Batteries, JOM 69 (2017) 1484-1496. https://doi.org/10.1007/s11837-017-2404-9

[5] Y. Liu, R. Zhang, J. Wang, Y. Wang, Current and future lithium-ion battery manufacturing, iScience 14 (2021) 102332. https://doi.org/10.1016/j.isci.2021.102332

[6] X.K. Lu, S.R. Daemi, A. Bertei, M.D.R. Kok, K.B. O'Regan, L. Rasha, J. Park, G. Hinds, E. Kendrick, D.J.L. Brett, P.R. Shearing, Microstructural Evolution of Battery Electrodes During Calendering, Joule 4 (2020) 2746-2768. https://doi.org/10.1016/j.joule.2020.10.010

[7] H.X. Kang, C. Lim, T.Y. Li, Y. Fu, B. Yan, N. Houston, V. de Andrade, F. de Carlo, L. Zhu, Geometric and Electrochemical Characteristics of LiNi1/3Mn1/3Co1/3O2 Electrode with Different Calendering Conditions, Electrochim. Acta 232 (2017) 431-438. https://doi.org/10.1016/j.electacta.2017.02.151

[8] R. Sim, S. Lee, W.D. Li, A. Manthiram, Influence of Calendering on the Electrochemical Performance of LiNi0.9Mn0.05Al0.05O2 Cathodes in Lithium-Ion Cells, ACS Appl. Mater. Interfaces 13 (2021) 42898-42908. https://doi.org/10.1021/acsami.1c12543

[9] J. Zhu, W. Li, T. Wierzbicki, Y. Xia, J. Harding, Deformation and failure of lithium-ion batteries treated as a discrete layered structure, Int. J. Plast. 121 (2019) 293-311. https://doi.org/10.1016/j.ijplas.2019.06.011

[10] A. Kwade, W. Haselrieder, R. Leithoff, A. Modlinger, F. Dietrich, K. Droeder, Current status and challenges for automotive battery production technologies, Nat. Energy 3 (2018) 290-300. https://doi.org/10.1038/s41560-018-0130-3

[11] D.L. Wood, J. Li, C. Daniel, Prospects for reducing the processing cost of lithium ion batteries, J. Power Sources 275 (2015) 234-242. https://doi.org/10.1016/j.jpowsour.2014.11.019

[12] T. Guenther, D. Schreiner, A. Metkar, C. Meyer, Classification of Calendering-Induced Electrode Defects and Their Influence on Subsequent Processes of Lithium-Ion Battery Production, Energy Technol. 8 (2020). https://doi.org/10.1002/ente.201900026

[13] D. Mayer, A.-K. Wurba, B. Bold, J. Bernecker, A. Smith, J. Fleischer, Investigation of the Mechanical Behavior of Electrodes after Calendering and Its Influence on Singulation and Cell Performance, Processes 9 (2021). https://doi.org/10.3390/pr9112009

[14] D. Mayer, J. Fleischer, Concept for modelling the influence of electrode corrugation after calendering on stacking accuracy in battery cell production, Procedia CIRP 104 (2021) 744-749. https://doi.org/10.1016/j.procir.2021.11.125

[15] A. Mayr, D. Schreiner, B. Stumper, R. Daub, In-line Sensor-based Process Control of the Calendering Process for Lithium-Ion Batteries, Procedia CIRP 107 (2022) 295-301. https://doi.org/10.1016/j.procir.2022.04.048

[16] D. Schreiner, M. Oguntke, T. Günther, G. Reinhart, Modelling of the Calendering Process of NMC-622 Cathodes in Battery Production Analyzing Machine/Material–Process–Structure Correlations, Energy Technol. 7 (2019) 1900840. https://doi.org/10.1002/ente.201900840

[17] D. Schreiner, T. Zünd, F.J. Günter, L. Kraft, B. Stumper, F. Linsenmann, M. Schüßler, R. Wilhelm, A. Jossen, G. Reinhart, H.A. Gasteiger, Comparative Evaluation of LMR-NCM and NCA Cathode Active Materials in Multilayer Lithium-Ion Pouch Cells: Part I. Production, Electrode Characterization, and Formation, J. Electrochem. Soc. 168 (2021) 030507. https://doi.org/10.1149/1945-7111/abe50c

[18] E.N. Primo, M. Chouchane, M. Touzin, P. Vazquez, A.A. Franco, Understanding the calendering processability of Li(Ni0.33Mn0.33Co0.33)O2-based cathodes, J. Power Sources 488 (2021) 229361. https://doi.org/10.1016/j.jpowsour.2020.229361

[19] E.N. Primo, M. Touzin, A.A. Franco, Calendering of Li(Ni0.33Mn0.33Co0.33)O2-Based Cathodes: Analyzing the Link Between Process Parameters and Electrode Properties by Advanced Statistics, Batteries & Supercaps 4 (2021) 834-844. https://doi.org/10.1002/batt.202000324

[20] A. Diener, S. Ivanov, W. Haselrieder, A. Kwade, Evaluation of Deformation Behavior and Fast Elastic Recovery of Lithium-Ion Battery Cathodes via Direct Roll-Gap Detection During Calendering, Energy Technol. 10 (2022). https://doi.org/10.1002/ente.202101033

[21] C. Zhang, S. Santhanagopalan, M.A. Sprague, A.A. Pesaran, Coupled mechanical-electrical-thermal modeling for short-circuit prediction in a lithium-ion cell under mechanical abuse, J. Power Sources 290 (2015) 102-113. https://doi.org/10.1016/j.jpowsour.2015.04.162

[22] C. Zhang, J. Xu, L. Cao, Z. Wu, Constitutive behavior and progressive mechanical failure of

electrodes in lithium-ion batteries, J. Power Sources 357 (2017) 126-137. https://doi.org/10.1016/j.jpowsour.2017.04.103

[23] P. Gupta, İ.B. Üçel, P. Gudmundson, E. Olsson, Characterization of the Constitutive Behavior of a Cathode Active Layer in Lithium-Ion Batteries Using a Bending Test Method, Exp. Mech. 60 (2020) 847-860. https://doi.org/10.1007/s11340-020-00613-5

[24] C. Meyer, H. Bockholt, W. Haselrieder, A. Kwade, Characterization of the calendering process for compaction of electrodes for lithium-ion batteries, J. Mater. Process. Technol. 249 (2017) 172-178. https://doi.org/10.1016/j.jmatprotec.2017.05.031

[25] C. Meyer, M. Kosfeld, W. Haselrieder, A. Kwade, Process modeling of the electrode calendering of lithium-ion batteries regarding variation of cathode active materials and mass loadings, J. Energy Storage 18 (2018) 371-379. https://doi.org/10.1016/j.est.2018.05.018

[26] J. Zhu, W. Li, Y. Xia, E. Sahraei, Testing and Modeling the Mechanical Properties of the Granular Materials of Graphite Anode, J. Electrochem. Soc. 165 (2018) A1160-A1168. https://doi.org/10.1149/2.0141807jes

[27] E. Sahraei, R. Hill, T. Wierzbicki, Calibration and finite element simulation of pouch lithium-ion batteries for mechanical integrity, J. Power Sources 201 (2012) 307-321. https://doi.org/10.1016/j.jpowsour.2011.10.094

[28] E. Sahraei, E. Bosco, B. Dixon, B. Lai, Microscale failure mechanisms leading to internal short circuit in Li-ion batteries under complex loading scenarios, J. Power Sources 319 (2016) 56-65. https://doi.org/10.1016/j.jpowsour.2016.04.005

[29] D. Schreiner, A. Klinger, G. Reinhart, Modeling of the Calendering Process for Lithium-Ion Batteries with DEM Simulation, Procedia CIRP 93 (2020) 149-155. https://doi.org/10.1016/j.procir.2020.05.158

[30] R. Ge, A.M. Boyce, Y. Shui Zhang, P.R. Shearing, D.J. Cumming, R.M. Smith, Discrete element method and electrochemical modelling of lithium ion cathode structures characterised by X-ray computed tomography, Chemical Eng. J. 465 (2023) 142749. https://doi.org/10.1016/j.cej.2023.142749

[31] A. Lundkvist, P.-L. Larsson, E. Olsson, A discrete element analysis of the mechanical behaviour of a lithium-ion battery electrode active layer, Powder Technol. 425 (2023) 118574. https://doi.org/10.1016/j.powtec.2023.118574

[32] C. Sangrós Giménez, B. Finke, C. Nowak, et al. Structural and mechanical characterization of lithium-ion battery electrodes via DEM simulations, Adv. Powder Technol. 29 (2018) 2312-2321. https://doi.org/10.1016/j.apt.2018.05.014

[33] A.C. Ngandjong, T. Lombardo, E.N. Primo, M. Chouchane, A. Shodiev, O. Arcelus, A.A. Franco, Investigating electrode calendering and its impact on electrochemical performance by means of a new discrete element method model: Towards a digital twin of Li-Ion battery manufacturing, J. Power Sources 485 (2021) 229320. https://doi.org/10.1016/j.jpowsour.2020.229320

[34] D. Mayer, B. Schwab, J. Fleischer, Influence of Electrode Corrugation after Calendering on the Geometry of Single Electrode Sheets in Battery Cell Production, Energy Technol. 11 (2023) 2200870. https://doi.org/10.1002/ente.202200870

[35] C.G. Wang, H.F. Tan, X.W. Du, Z.M. Wan, Wrinkling prediction of rectangular shell-membrane under transverse in-plane displacement, Int. J. Solids Struct. 44 (2007) 6507-6516. https://doi.org/10.1016/j.ijsolstr.2007.02.036